Analytical analysis of second-order Stokes wave in Brillouin ring fiber laser

H. A. Al-Asadi,[1] M. H. Abu Bakar,[1] M. H. Al-Mansoori,[2] F. R. Mahamd Adikan,[3] and M. A. Mahdi[1,*]

[1]*Wireless and Photonics Networks Research Center, Faculty of Engineering,Universiti Putra Malaysia, 43400 UPM Serdang, Selangor, Malaysia*

[2]*Faculty of Engineering, Sohar University, P.O Box 44, Sohar P.C. 311, Sultanate of Oman*

[3]*Department of Electrical Engineering, Faculty of Engineering, University of Malaya, 50603, Kuala Lumpur, Malaysia*

[*]*mdadzir@eng.upm.edu.my*

Abstract: This paper details a theoretical modeling of Brillouin ring fiber laser which incorporates the interaction between multiple Brillouin Stokes signals. The ring cavity was pumped at several Brillouin pump (BP) powers and the output was measured through an optical coupler with various coupling ratios. The first-order Brillouin Stokes signal was saturated with the presence of the second-order Stokes signal in the cavity as a result of energy transfer between them. The outcome of the study found that the optimum point for the first-order Stokes wave performance is at laser power reduction of 10%. Resultantly, at the optimum output coupling ratio of 90%, the BFL was able to produce 19.2 mW output power at BP power and Brillouin threshold power of 60 and 21.3 mW respectively. The findings also exhibited the feasibility of the theoretical models application to ring-type Brillouin fiber laser of various design parameters.

OCIS codes: (190.4370) Nonlinear optics, fibers; (190.5890) Scattering, stimulated; (290.5900) Scattering, stimulated Brillouin.

References and links

1. M. F. Ferreira, J. F. Rocha, and J. L. Pinto, "Analysis of the gain and noise characteristics of fiber Brillouin amplifiers," Opt. Quantum Electron. **26**(1), 35–44 (1994).
2. S. P. Smith, F. Zarinetchi, and S. Ezekiel, "Narrow-linewidth stimulated Brillouin fiber laser and applications," Opt. Lett. **16**(6), 393–395 (1991).
3. K. Schneider and S. Schiller, "Narrow-linewidth, pump-enhanced singly-resonant parametric oscillator pumped at 532 nm," Appl. Phys. (Berl.) **65**(6), 775–777 (1997).
4. J. Geng, S. Staines, Z. Wang, J. Zong, M. Blake, and S. Jiang, "Highly stable low-noise Brillouin fiber laser with ultranarrow spectral linewidth," IEEE Photon. Technol. Lett. **18**(17), 1813–1815 (2006).
5. G. P. Agrawal, *Nonlinear Fiber Optics* (Academic Press, 2007).
6. T. A. Haddud, M. H. Al-Mansoori, A. K. Zamzuri, S. Shaharudin, M. K. Abdullah, and M. A. Mahdi, "24-Line of Brillouin-erbium fiber laser utilizing a Fabry-Perot cavity in L-band," Microw. Opt. Technol. Lett. **45**(2), 165–167 (2005).
7. M. H. Al-Mansoori, M. A. Mahdi, and M. Premaratne, "Novel multiwavelength L-band Brillouin-Erbium fiber laser utilizing double-pass Brillouin pump preamplified technique," IEEE J. Sel. Top. Quantum Electron. **15**(2), 415–421 (2009).
8. M. H. Al-Mansoori and M. A. Mahdi, "Multiwavelength L-band Brillouin-erbium comb fiber laser utilizing nonlinear amplifying loop mirror," J. Lightwave Technol. **27**(22), 5038–5044 (2009).
9. T. H. Russell, W. B. Roh, and J. R. Marciante, "Incoherent beam combining using stimulated Brillouin scattering in multimode fibers," Opt. Express **8**(4), 246–254 (2001).
10. B. C. Rodgers, T. H. Russell, and W. B. Roh, "Laser beam combining and cleanup by stimulated Brillouin scattering in a multimode optical fiber," Opt. Lett. **24**(16), 1124–1126 (1999).
11. T. H. Russell and W. B. Roh, "Threshold of the second Stokes scattering in a fiber stimulated Brillouin scattering beam combiner," in *Conference Proceedings - Lasers and Electro-Optics Society Annual Meeting-LEOS* (2001), 665–666.
12. K. D. Park, H. Ryu, W. K. Lee, S. K. Kim, H. S. Moon, and H. S. Suh, "Threshold features of a Brillouin Stokes comb generated in a distributed fiber Raman amplifier," Opt. Lett. **28**(15), 1311–1313 (2003).

#156275 - $15.00 USD Received 11 Oct 2011; revised 17 Nov 2011; accepted 21 Nov 2011; published 1 Dec 2011

13. D. Zhang, X. Zhang, X. Li, A. Xu, Z. Wang, F. Zhang, and Z. Chen, "Stimulated Brillouin scattering and Rayleigh cooperative process in 300 Km optical transmission," Microw. Opt. Technol. Lett. **49**(12), 2939–2941 (2007).
14. N. F. P. Zel'dovich and V. V. Shkunov, *Principles of Phase Conjugation* (Springer-Verlag, Berlin, 1985).
15. N. A. M. A. Hambali, M. A. Mahdi, M. H. Al-Mansoori, M. I. Saripan, A. F. Abas, and M. Ajiya, "Effect of output coupling ratio on the performance of ring-cavity Brillouin fiber laser," Laser Phys. **20**(7), 1618–1624 (2010).

1. Introduction

The rise of optical systems as the premier communication networks has attracted a lot of interest in fiber lasers. Fiber lasers are highly sought after due to their capability as highly efficient and robust optical sources. One of the most popular methods of generating fiber lasers is by taking advantage of a nonlinear effect called stimulated Brillouin scattering (SBS). The utilization of SBS in Brillouin fiber laser (BFL) is not only limited to optical communication sources but has also been employed in various other applications such as narrow-bandwidth amplification [1], fiber-optic sensors [2], high-resolution spectroscopy [3], and interferometer sensing [4].

SBS occurs due to the formation of an index grating in the fiber, which resulted from the generation of acoustic waves by the pump light [5]. Consequently, the 1st-order Brillouin Stokes wave is created through backscattering of light at a downshifted frequency. The 1st Stokes oscillates in the cavity and once it reaches a certain threshold, the same process repeats again thus generating another Stokes signal in the opposite direction. This became the basis of multiwavelength laser, which is a very well known application of BFL. The integration of BFL with erbium is a popular choice due to the higher amplification accorded by the gain medium, which allows for higher Stoke power and consequently simplifying the generation of subsequent Stokes signals. Work on this Brillouin-erbium fiber laser (BEFL) has found up to 24 channels in a general linear cavity design [6]. BEFL in a novel amplifying loop design was able to generate 27 Stokes signal in the L-band region [7]. The tuning range of multiwavelength BEFL can be further enhanced by using a double-pass pre-amplification technique as reported in [8].

Besides the generation of multiwavelength lasers, BFL can be used for single-wavelength lasers as well. There are some processes that depend solely on first-order Brillouin Stokes wave such as incoherent beam combining [9] and beam cleanup [10]. Nevertheless, while the multiwavelength BFL revels in the generation of higher order Stokes, the production of single-wavelength BFL is hampered by this natural phenomenon as the energy from the first-order Stokes wave would be reduced and transferred to the second-order Stokes wave. As a result, single-wavelength BFL devices normally operate below their maximum capabilities in order not to exceed the threshold of the second-order Stokes signal.

Studies have been performed to study the threshold features of the second-order Stokes wave in several devices. While Russell and Roh concluded that second-order SBS was not a limiting factor in beam combiner [11], considerable power reduction was reported in the first-order Stokes signal due to the presence of higher order SBS component in distributed Raman amplifiers [12] and long distance all-Raman transmission system [13]. No study however, has ever been conducted to estimate the optimum point to achieve maximum first-order Brillouin Stokes wave performance with the presence of second-order Stokes signal.

In this paper, we present an analytical model for the analysis of second-order Stokes wave of a continuous wave operation of a ring-cavity BFL. Using the analytical approach for the model allows the study of the ring laser behavior with the presence of the second-order Stokes wave, for the first time, to the best of our knowledge. A theoretical model was used to predict the best parameters to achieve optimum laser performance. Investigation was done on the effect of second-order Stokes wave for the performance of BFL at various output coupling ratios.

#156275 - $15.00 USD Received 11 Oct 2011; revised 17 Nov 2011; accepted 21 Nov 2011; published 1 Dec 2011

2. Modeling of ring cavity BFL

The schematic diagram of BFL considered for the analytical simulation and used for experimental verification is depicted in Fig. 1. The configuration comprised of an external narrow-linewidth tunable laser source (TLS), an erbium-doped fiber amplifier (EDFA), a section of dispersion compensating fiber (DCF), an optical circulator and a tunable coupler. The EDFA gain block consisted of an erbium-doped fiber (EDF) of 8 meters long and wavelength division multiplexing (WDM) coupler. The EDF was pumped by a 1480 nm laser diode for the amplification of seed signal from TLS to be used as the Brillouin pump (BP) signal prior to entering the ring cavity.

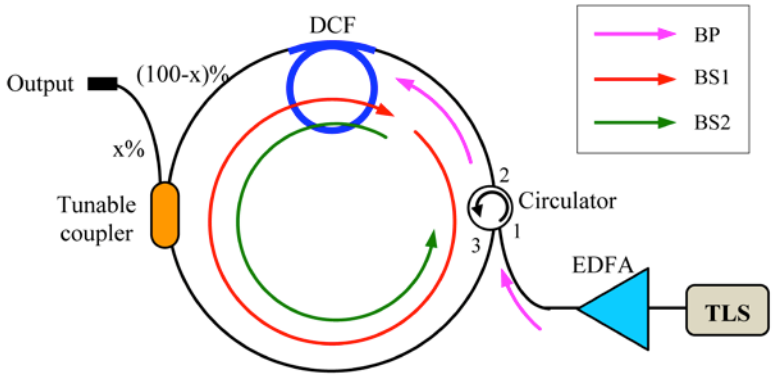

Fig. 1. Schematic diagram for BFL. BS1 and BS2 denote the first- and second-order Stokes waves correspondingly.

This amplified narrow linewidth BP was injected into the DCF through port 1 to port 2 of the optical circulator. The optical circulator was also used to force unidirectional operation of the laser in the cavity. When the power of BP signal overcomes the threshold condition in DCF, a Stokes signal occurs at a lower frequency of approximately 11 GHz downshifted from the BP. The small DCF core induced higher nonlinearity effects that lowered the SBS threshold and allowed the generation of higher-order Stokes at lower BP power. This first-order Stokes signal then propagated inside the ring cavity through port 2 to port 3 of the optical circulator to form a laser. The circulating signal was taken out at the x% leg of the tunable coupler. This output coupling ratio (x) was varied from 10 to 95% to analyze the laser performance at different circulating power in the cavity.

In general thumb rule of laser, by further increasing the BP power, the amount of Stokes laser power was also increased. Under this circumstance, the first-order Stokes wave shown in Fig. 1 that propagated in the clockwise direction could also generate a second-order Stokes signal when its SBS threshold was met. This new signal propagated in the opposite direction of the first-order Stokes wave (anti clockwise direction). Subsequently, the energy of the initial Stokes wave was transferred to the new Stokes signal at the expense of the first-order Stokes signal performance degradation. This transition phase is our main research objective because the linear response of laser (in case of first-order Stokes wave) is no longer obeyed. The impact of the second-order Stokes wave presence is taken into our theoretical model to determine the performance characteristics of the first-order Stokes wave. In our experiment, the use of circulator limited the setup to a unidirectional operation, thus the second-order Stokes wave could not circulate and initiate its lasing process. Additionally, the unidirectional operation prohibited the second-order Stokes signal from being detected at the output; therefore, the Rayleigh backscattering component of the Stokes signal was observed instead in order to assess its evolution in the cavity.

#156275 - $15.00 USD Received 11 Oct 2011; revised 17 Nov 2011; accepted 21 Nov 2011; published 1 Dec 2011

Steady state differential equations including the effect of SBS in ring cavity BFL, can be represented by three waves mixing and absorptions on the coupling between the wave powers of BP, first-order Stokes signal, BS1 and second-order Stokes signal, BS2 as given by [14];

$$\frac{\partial P_{BP}(z)}{\partial z} = \left(-\frac{g_B(v)}{A_{eff}} P_{BS1}(z) - \left(\alpha_{12}\alpha_{sp}\alpha_c\alpha_f k \right) \right) P_{BP}(z), \tag{1a}$$

$$\frac{\partial P_{BS1}(z)}{\partial z} = \left(-\frac{g_B(v)}{A_{eff}} P_{BP}(z) - \left(\alpha_{23}\alpha_{sp}\alpha_c\alpha_f (1-k) \right) \right) \text{a } P_{BS1}(z), \tag{1b}$$

$$\frac{\partial P_{BS2}(z)}{\partial z} = \left(\frac{g_B(v)}{A_{eff}} P_{BS1}(z) - \left(\alpha_{12}\alpha_{sp}\alpha_c\alpha_f k \right) \right) P_{BS2}(z), \tag{1c}$$

where, α_{12} and α_{23} represent the loss factors of the optical circulator between ports 1 and 2, and ports 2 and 3, respectively. We introduced α_c and α_f as the coupler loss and total loss of DCF, respectively. α_{sp} is the coefficient of the loss intensity due to a splice in a ring cavity and k is the output coupling coefficient. A_{eff} is the effective cross section area and g_B is the Brillouin gain coefficient.

The wave power at the output coupler ports are interrelated as

$$P_{out}(z) = k(1-\gamma) P_{BS1}(z), \tag{2}$$

where γ is the intensity loss coupler coefficient.

Since the depletion of the backward propagating Stokes wave was ignored, the full analytical solutions to Eqs. (1a), (1b) and (1c) are given by,

$$P_{BP}(z) = P_{BP}(0) \exp(-\alpha_{12}\alpha_{sp}\alpha_c\alpha_f kz), \tag{3a}$$

$$P_{BS1}(z) = P_{BS1}(L) \exp\left(\frac{1}{\alpha_{12}\alpha_{sp}\alpha_c\alpha_f kA_{eff}} \begin{pmatrix} P_{BP}(0) g_B \left(e^{-\alpha_{12}\alpha_{sp}\alpha_c\alpha_f kz} - e^{-\alpha_{12}\alpha_{sp}\alpha_c\alpha_f kL} \right) \\ -\alpha_{12}\alpha_{23}\alpha_{sp}^2\alpha_c^2\alpha_f^2 k(k-1) A_{eff}(L-z) \end{pmatrix} \right), \tag{3b}$$

$$P_{BS2}(z) = P_{BS2}(0) \exp\left(\frac{1}{2\alpha_{12}^2\alpha_{sp}^2\alpha_c^2\alpha_f^2 k^2 A_{eff}^2} \begin{pmatrix} 2g_B^2 P_{BS1}(L) P_{BP}(0) \left(e^{-\alpha_{12}\alpha_{sp}\alpha_c\alpha_f kz} - \alpha_{12}\alpha_{sp}\alpha_c\alpha_f kz e^{-\alpha_{12}\alpha_{sp}\alpha_c\alpha_f kL} \right) \\ -2g_B P_{BS1}(L) \begin{pmatrix} -g_B P_{BP}(0) + \\ A_{eff}\alpha_{12}^2\alpha_{sp}^2\alpha_c^2\alpha_f^2 k^2 z \left(\alpha_{23}\alpha_{sp}\alpha_c\alpha_f (k-1)(L-\frac{z}{2}) \right) - 1 \end{pmatrix} \\ -2\alpha_{12}^3\alpha_{sp}^3\alpha_c^3\alpha_f^3 k^3 A_{eff}^2 z \end{pmatrix} \right), \tag{3c}$$

where, $P_{BP}(0)$, $P_{BS1}(L)$ and $P_{BS2}(0)$ represent the BP power coupled in the ring cavity through ports 1 and 2 of optical circulator, the initial values of first-order Stokes wave at $z = L$ and the second-order Stokes wave at $z = 0$ of optical fiber ring cavity, correspondingly.

Substituting Eqs. (3a) and (3b) in Eq. (2), we arrive at the solution for the output wave power as a function of fiber length in ring cavity BFL in the form,

$$P_{out}(z) = k(1-\gamma) P_{BS1}(L) \exp\left(\frac{1}{\alpha_{12}\alpha_{sp}\alpha_c\alpha_f kA_{eff}} \begin{pmatrix} P_{BP}(0) g_B \left(e^{-\alpha_{12}\alpha_{sp}\alpha_c\alpha_f kz} - e^{-\alpha_{12}\alpha_{sp}\alpha_c\alpha_f kL} \right) \\ -\alpha_{12}\alpha_{23}\alpha_{sp}^2\alpha_c^2\alpha_f^2 k(k-1) A_{eff}(L-z) \end{pmatrix} \right), \tag{4}$$

#156275 - $15.00 USD Received 11 Oct 2011; revised 17 Nov 2011; accepted 21 Nov 2011; published 1 Dec 2011

3. Ring cavity BFL simulation results

The BFL analytical model requires input data that can be obtained through experimental configuration [15]. The BFL setup characteristics are listed in Table 1. The loss coefficient and effective area, together with other fiber parameters, the pump powers and the ratio of the optical coupler, represent the input data for the simulation results. The modeled BFL have the loss factors of optical circulator between ports 1 and 2 and ports 2 and 3, α_{12} =0.8 dB and α_{23} =0.7 dB, respectively and α_{sp} =0.3 dB. The schematic of the ring cavity BFL considered for simulation results and used for experimental verification is depicted in Fig. 1.

Table 1. Parameters used in the simulation work.

Parameter	Value
DCF fiber length	11 km
DCF effective area	20 μm^2
DCF total loss	7.3 dB
Brillouin gain coefficient	1.12×10^{-11} m/W
Tunable coupler insertion loss	0.5 dB
Temperature coefficient of refractive index	3.97×10^{-4}
Nonlinear coefficient	7.31 $(Wkm)^{-1}$
Total dispersion	−1328 ps/nm

Simulation results were compared to the experiment data obtained during the steady state for verification of our analytical model. The ring cavity was pumped at several BP power from 0 mW up to the maximum EDFA output of 24 mW with variations to the output coupling ratio.

Figure 2 depicts the comparison between the theoretical results to the experimental output, which validates the analytical models used in this study. At 10% output coupling ratio, less than 2 mW of Stokes signal power was observed since 90% of the output power continued to propagate inside the cavity. Lasing can only occur when the cavity gain from SBS effect is equal to the cavity loss at the threshold condition. The lower output coupling ratio resulted in lower cavity loss and in turn reduced the BP power required to reach the threshold condition. Consequently, the Brillouin threshold for this output coupling ratio can be reached at low BP power of 0.9 mW. By increasing the output coupling ratio from 10% to 95%, the amount of cavity loss can also be elevated and at the highest output coupling ratio of 95%, the Brillouin threshold was higher as well, measuring at 2.6 mW. However, the highest Stokes signal power of 7.3 mW was not attained from the highest output coupling ratio but instead from the 90% output coupling ratio at BP power of 24 mW.

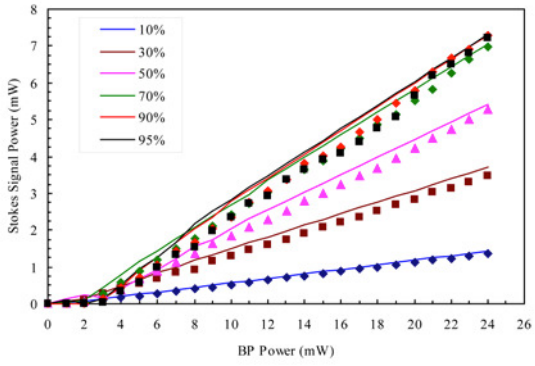

Fig. 2. Theoretical (solid) and experimental (dash) results Brillouin output power of ring cavity BFL for various coupling ratio of optical coupler.

#156275 - $15.00 USD Received 11 Oct 2011; revised 17 Nov 2011; accepted 21 Nov 2011; published 1 Dec 2011

Figure 3 illustrates the BFL optimum output Stokes power as a function of coupling ratio with 11 km long DCF. Also, it shows that as the coupling ratio was increased from 10% to 95%, the optimum Brillouin output power of BFL also rose until 90% reached 7.2 mW. When the coupling ratio is 95%, the optimum Brillouin output power decreased to 7.1 mW. This was due to the gain saturation which led to less available gain for amplification of the first-order Stokes wave and thus as a result, lower output powers were detected. The simulation results of our BFL analytical model show good comparison to the experimental data. Experimental observations at the output showed no Rayleigh backscattering component of BS2 present at BP less than 25 mW thus the effect of higher orders Stokes wave was assumed to be of minimal significance to the overall output of the laser. In the following paragraphs, this effect was considered to further evaluate the performance of single wavelength BFL.

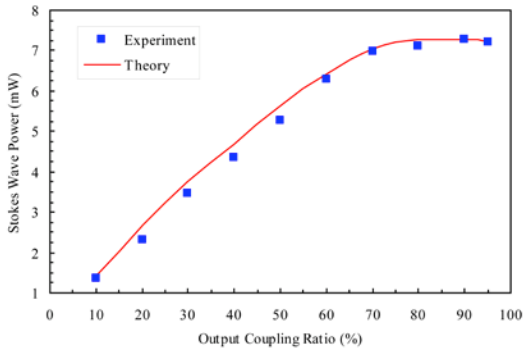

Fig. 3. Theoretical and experimental data on optimum Brillouin output power of ring cavity BFL for various coupling ratios of optical coupler.

After increasing the BP power, the backward propagating first-order Stokes wave reached the threshold for second-order Stokes wave generation in forward direction. Figure 4 demonstrates the theoretical power distribution of the first- and second-order Stokes waves as a function of BP power. As the validity of the analytical models was already proven by Fig. 2 and Fig. 3, the models were then applied for theoretical BP power higher than 24 mW. Higher order Stokes waves can be expected from BFL if the BP power pushed further than 100 mW. Our model can be used to predict the performance of BFL with the presence of second-order Stokes wave. At the lower BP power, the first-order Stokes wave increased linearly. The first-order Stokes laser output power reached 6.3 mW before the second-order Stokes wave was generated at the output coupling ratio of 50%. After reaching the threshold of the second-order Stokes wave, the first-order Stokes laser power started to decrease as represented by the red line in Fig. 4. In this simulation, the output power was saturated at 17.1 mW. The critical pump power in which the BS signal power started to saturate was measured around 83 mW pump power for 50% output coupling ratio. This saturation characteristic is the evidence of energy transfer from the first-order Stokes signal to the second-order Stokes signal, which propagated in the same direction of BP power. Moreover, this phenomenon was due to the decreasing round trip gain in ring cavity as the BP power level was increased thus resulting in gain saturation. Since the use of circulator blocked the second-order Stokes wave from travelling on a complete round-trip, it did not resonate as a laser mode and the BFL was locked to first-order Stokes wave.

#156275 - $15.00 USD Received 11 Oct 2011; revised 17 Nov 2011; accepted 21 Nov 2011; published 1 Dec 2011

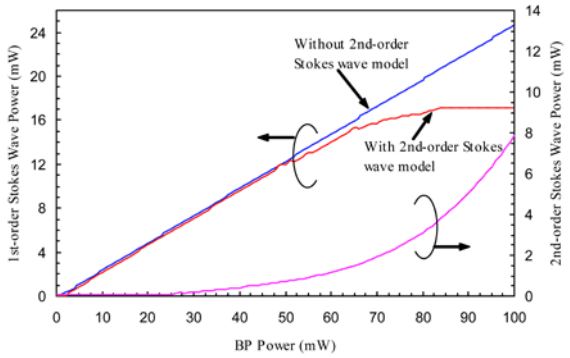

Fig. 4. Theoretical power distribution of the first- and second-order Stokes waves as a function of Brillouin pump power of ring cavity BFL at 50% coupling ratio.

Once above the threshold of the second-order Stokes signal generation, the increment of the BFL output power decreased as the BP power was added. Although the optimum operating condition can be defined at the second-order SBS threshold power, the output power at that condition was considerably low. As an example; referring to Fig. 4, the second-order SBS threshold power was about 21.3 mW and its corresponding output power was only 6.3 mW. In order to increase the output power, the optimum condition was determined when the output power with second-order Stokes signal was reduced by 10% from its output power without the presence of second-order Stokes wave. In this case, only 10% of powers were transferred to the second-order Stokes signal and the absolute output power was much higher as compared to the previous definition of optimum condition. This was possible as the energy transfer to the second-order Stokes wave was kept low and still allowed the first-order Stokes signal power to increase. As evidently seen in Fig. 4, the optimum BP power and output power at 10% output power reduction were 50 and 12.3 mW, respectively.

The amount of output power taken from the BFL system was dictated by the coupling ratio of the optical coupler used. Various coupling ratios have been used in our analytical modeling which yielded different output power. The coupling ratio dictated the tradeoff between the intra-cavity power and the output power. The optimum operating conditions of BFL for different output coupling ratios are shown in Fig. 5(a) and 5(b).

Obviously, from analytical results, the output power was increased with the increment of the output coupling ratio. This was owed to more energies decoupling from the cavity as a result of the output power increment. Meanwhile, the threshold of second-order Stokes wave was also increased as the coupling ratio increased. In this case, the circulating energies in the cavity decreased in tandem with the increment of coupling ratio. Therefore, higher BP powers were required to achieve the second-order SBS threshold. The same trend was followed by the optimum BP power. The saturated output power is plotted to indicate the difference between its value and the optimum output power. From Fig. 5(b), the percentage of the optimum output power to the saturated output power varied from 43% to 89% for the output coupling ratio from 10% to 90% respectively. The increment of this parameter is directly related to the amount of circulating energy in the cavity. For low output coupling ratio, most of the energy was circulated in the cavity that triggered the generation of second-order Stokes wave at lower threshold power. Owing to this effect, the energy transfer occurred earlier in which the efficiency was the lowest. On the other hand, the circulating energy was low for larger output coupling ratios and pushed the second-order SBS threshold higher. As a result, the energy transfer occurred later and the performance of the laser was enhanced, which translated to higher efficiency. These findings show that at the optimum coupling ratio of 90%, the optimum BP and output powers were 60 and 19.2 mW, respectively. Also, the

#156275 - $15.00 USD Received 11 Oct 2011; revised 17 Nov 2011; accepted 21 Nov 2011; published 1 Dec 2011

figures show that the BFL offered the highest output power (the first-order Stokes wave) before the second-order Stokes wave degraded the BFL efficiency.

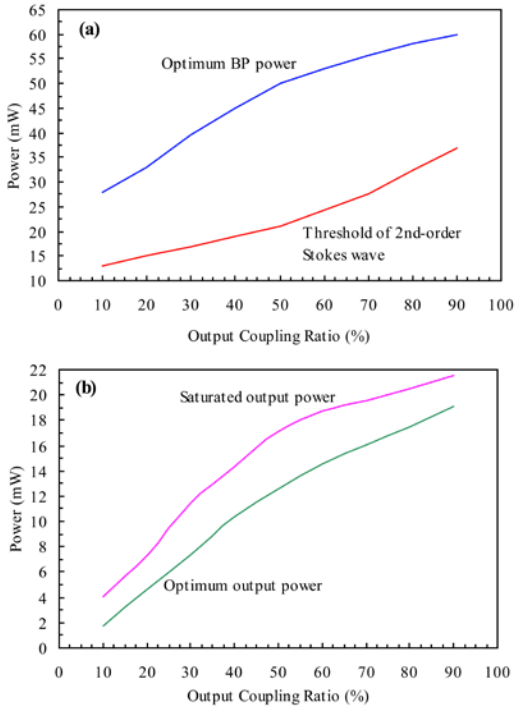

Fig. 5. Theoretical output power distribution of the BFL for various output coupling ratios; (a) threshold of second-order Stokes wave with the optimum BP power and (b) optimum and saturated output powers.

4. Conclusion

Theoretical models of Brillouin fiber laser in a ring cavity were developed in this study. Analytic solutions of steady state differential equations of the optical waves interaction including the effect of SBS in ring cavity BFL have been provided. Additionally, the comparison between the modeling results with experimental results was made and good agreement between those results was found. This validated the feasibility of the analytical models application to ring-type BFL with different design parameters. The maximum power of 7.3 mW for the output power was obtained at BP power of 24 mW and 90% coupling ratio and 11 km DCF optical fiber length. By further increasing the BP slightly up to 100 mW, the amount of Stokes signal power can be increased. However, the generation of the second-order Stokes wave must be considered in our developed model. Our findings showed that at the optimum coupling ratio of 90%, the second-order SBS threshold power, the optimum BP and output powers are 21.3, 60 and 19.2 mW, respectively. Based on these findings, an optimum operating condition was determined to ensure that the output power is still high and its energy transfer to second-order Stokes signal is kept low.

Acknowledgments

This work was partly supported by the Ministry of Higher Education, Malaysia and the Universiti Putra Malaysia under research grant # 05-01-10-0901RU and Graduate Research Fellowship.

#156275 - $15.00 USD Received 11 Oct 2011; revised 17 Nov 2011; accepted 21 Nov 2011; published 1 Dec 2011